


Article

Leveraging Bayesian Quadrature for Accurate and Fast Credit Valuation Adjustment Calculations

Noureddine Lehdili ^{*}, Pascal Oswald and Othmane Mirinioui

Market and Counterparty Risk Modeling (MCRM), Enterprise Risk Management Department (ERM), Natixis CIB, 75013 Paris, France; pascal.oswald@natixis.com (P.O.); othmane.mirinioui@dauphine.eu (O.M.)

* Correspondence: noureddine.lehdili@natixis.com

Abstract: Counterparty risk, which combines market and credit risks, gained prominence after the 2008 financial crisis due to its complexity and systemic implications. Traditional management methods, such as netting and collateralization, have become computationally demanding under frameworks like the Fundamental Review of the Trading Book (FRTB). This paper explores the combined application of Gaussian process regression (GPR) and Bayesian quadrature (BQ) to enhance the efficiency and accuracy of counterparty risk metrics, particularly credit valuation adjustment (CVA). This approach balances excellent precision with significant computational performance gains. Focusing on fixed-income derivatives portfolios, such as interest rate swaps and swaptions, within the One-Factor Linear Gaussian Markov (LGM-1F) model framework, we highlight three key contributions. First, we approximate swaption prices using Bachelier's formula, showing that forward-starting swap rates can be modeled as Gaussian dynamics, enabling efficient CVA computations. Second, we demonstrate the practical relevance of an analytical approximation for the CVA of an interest rate swap portfolio. Finally, the combined use of Gaussian processes and Bayesian quadrature underscores a powerful synergy between precision and computational efficiency, making it a valuable tool for credit risk management.

Keywords: credit valuation adjustment; expected exposure; Basel III; FRTB; potential future exposure; Gaussian process regression; machine learning; interest rate swaps

MSC: 91G20; 91B05; 62G08; 60G15; 65D05



Citation: Lehdili, N.; Oswald, P.; Mirinioui, O. Leveraging Bayesian Quadrature for Accurate and Fast Credit Valuation Adjustment Calculations. *Mathematics* **2024**, *12*, 3779. <https://doi.org/10.3390/math12233779>

Academic Editor: Luca Piccoli

Received: 16 October 2024

Revised: 23 November 2024

Accepted: 27 November 2024

Published: 29 November 2024



Copyright: © 2024 by the authors. Licensee MDPI, Basel, Switzerland. This article is an open access article distributed under the terms and conditions of the Creative Commons Attribution (CC BY) license (<https://creativecommons.org/licenses/by/4.0/>).

1. Introduction

Counterparty risk is one of the most complex types of financial risk to measure and manage, as it results from the interaction between market risk and credit risk, and is also influenced by systemic factors such as the failure of large institutions [1–3]. This risk is particularly relevant for over-the-counter (OTC) derivatives and has gained in importance since the global financial crisis [4–6]. Prior to the 2008 financial crisis, numerous financial institutions addressed counterparty credit risk by engaging exclusively with the most stable counterparties, frequently trusting the presumed solvency of entities considered “too big to fail.” Nonetheless, the crisis exposed that these very institutions often represented the greatest counterparty risk. Counterparty risk arises from the combination of market risk, which determines exposure, and credit risk, which assesses the creditworthiness of the counterparty. It is not always clear whether a counterparty with a high probability of default but low exposure is preferable to one with higher exposure but a lower default probability. Credit valuation adjustment (CVA) provides a precise measure of counterparty risk and enables a numerical distinction between these different scenarios. It assesses the counterparty risk faced by an institution, providing the opportunity for it to be managed, traded, or hedged effectively [1,7–9]. The precise and efficient calculation of counterparty credit risk metrics, such as credit valuation adjustment (CVA), value at risk (VaR), and

expected shortfall (ES) [10–14], remains a significant challenge for financial institutions. While traditional methods are reliable, they are often computationally costly and face difficulties when scaling for complex portfolios, especially those containing exotic derivatives like Bermudan swaptions. These limitations can impede timely risk assessment, a growing necessity under regulatory frameworks like Basel III [4,5,15,16]. This research aims to bridge this gap by examining how advanced statistical techniques—particularly Gaussian process regression (GPR) and Bayesian quadrature—can improve both the accuracy and efficiency of risk metric calculations. The underlying motivation is the increasing demand for financial institutions to adopt cutting-edge tools that provide faster, more dependable risk evaluations. This approach offers the potential for substantial cost reductions while ensuring compliance with evolving regulatory demands, making it a promising solution for contemporary risk management. Various strategies are employed to mitigate counterparty risk in OTC derivatives. Netting agreements involve legally binding arrangements that offset the positive and negative exposures between counterparties. By consolidating multiple transactions into a single net position, netting reduces the overall credit exposure between the parties. Netting agreements serve to reduce counterparty credit risk by minimizing the outstanding amounts that must be settled between parties in the event of a default. Collateralization requires counterparties to post collateral, providing a buffer against potential losses. The Credit Support Annex (CSA [17]) outlines terms for collateralization and margin requirements, further securing transactions. Additionally, hedging with credit derivatives, such as credit default swaps (CDSs), transfers the risk to third parties, protecting against defaults. These combined approaches enhance risk management and financial stability.

Counterparty risk metrics must be evaluated for economic, accounting, and regulatory purposes. The economic approach calculates potential future exposure (PFE) to set exposure limits. The accounting approach incorporates value adjustments (XVAs), particularly CVA, into pricing. The regulatory approach assesses the capital needed to cover unexpected losses, such as EEPE and VaR-CVA. Exposure, essential in these three approaches, requires rapid and accurate estimates. Banks use Monte Carlo simulations and pricing libraries to evaluate portfolios, leading to complex and time-consuming processes, especially under the new regulations. To overcome these challenges, institutions are increasingly adopting approximations [8,18–20] and machine learning methods [21,22] such as deep learning algorithms [21,23–28], to reduce computational complexity while maintaining accuracy.

1.1. Research Focus and Contributions

In this paper, we specifically focus on the application of these techniques for calculating counterparty credit risk metrics to address the following question: How can we efficiently implement these risk metrics, reducing computation time while ensuring satisfactory accuracy? In the academic and professional literature, deep learning and Gaussian process regression are used to accurately and quickly value derivatives [19,23,29,30]. Another potential application involves using Gaussian processes to estimate the value at risk (VaR) and the expected shortfall for market risk measurement [28,31,32]. In addition, other machine learning applications, such as those based on neural networks and Chebyshev tensors, are utilized to compute risk metrics [16,33]. In this research, we investigated the application of Gaussian process regression (GPR) and Bayesian quadrature to tackle the computational challenges associated with the evaluation of counterparty credit risk (CCR) metrics, with a particular emphasis on credit valuation adjustment (CVA). This study introduced a novel framework designed to overcome the issues of computational complexity and precision in CCR metric estimation. Using advanced statistical methods within the robust LGM-1F model, we provide a more efficient and precise approach to managing counterparty credit risk in portfolios of fixed-income derivatives.

Our methodology capitalizes on the strengths of Bayesian quadrature, a GPR-based technique, to compute numerical integrals with minimal observations. GPR possesses unique mathematical advantages, such as rapid and numerically stable evaluations and exponential convergence to the target function when dealing with analytically well-defined

functions. These attributes make GPR a powerful tool for approximating complex functions, particularly in derivative pricing and risk assessment. By integrating Bayesian quadrature into this framework, we enable efficient and accurate CVA computations, significantly reducing computational time without sacrificing precision.

A key feature of our approach is that the training phase of the algorithm for estimating prices is carried out at the portfolio level, aggregated by counterparty, rather than on a deal-by-deal basis. This unique methodology improves both the efficiency and performance of the model, offering a significant advantage over conventional techniques that assess individual transactions.

The scope of this work focuses on fixed-income derivative portfolios comprising interest rate swaps, swaptions, and cancellable swaps, all modeled within the One-Factor Linear Gaussian Markov (LGM-1F) framework. This widely recognized model serves as the benchmark for evaluating and managing the risks of such derivatives, ensuring consistency across valuation, risk management, and credit risk assessment.

This paper delivers three key contributions:

- **Pricing Approximation:** Using Bachelier's formula, we demonstrate that forward start rates can be effectively modeled as Gaussian processes, enabling efficient and accurate CVA calculations.
- **Practical CVA Approximations:** We propose and validate an analytical approximation for the CVA of an interest rate swap portfolio, simplifying the calculation process while maintaining accuracy.
- **Synergy of GPR and Bayesian Quadrature:** Using GPR's functional approximation capabilities along with Bayesian quadrature optimization of numerical integration, we achieve an innovative balance between computational efficiency and precision, presenting a practical solution for credit risk management.

1.2. Paper Structure

The structure of this paper is organized as follows: Section 2 provides an overview of the risk measures of counterparty credit, introducing key metrics such as expected exposure and credit valuation adjustment (CVA), which are used to quantify the risk of counterparty credit. Section 3 discusses Bayesian inference modeling, offering an introduction to Gaussian process regression (GPR), training algorithms, and the concept of Bayesian quadrature. Section 4 focuses on the calculation of CVA in the LGM-1F model, where analytical CVA approximations are explored, along with swap valuation techniques within the LGM-1F framework. Section 5 presents numerical applications for CVA calculation, detailing convergence tests for interest rate swaps, classical CVA calculation approaches, and numerical results obtained using GPR and Bayesian quadrature. Finally, Sections 6 and 7 provide the conclusions and discussion, summarizing the key findings and suggesting future research directions.

2. Counterparty Credit Risk Measures

In this section, we introduce the fundamental concepts and notations related to counterparty credit risk (CCR), credit exposures, and credit valuation adjustment (CVA). Counterparty credit risk (CCR) refers to the possibility that a counterparty may default or fail to fulfill its financial obligations before the settlement of derivative payments. A financial loss occurs if, at the time of default, the derivative held by the counterparty has a positive economic value for the financial institution [2,4]. Unlike traditional loans, where only the lender might incur a loss, CCR impacts both counterparties: the market value can be either positive or negative for each, and it may fluctuate over time due to changing market conditions. The counterparty exposure, denoted as $E(t)$, represents the potential financial loss that the financial institution could face at time t across all outstanding derivative transactions with the counterparty, assuming the counterparty defaults at that moment and accounting for netting and collateral but excluding any potential recoveries [34].

2.1. Expected Exposure

Consider a portfolio consisting of N derivative transactions between a financial institution and a given counterparty. The counterparty experiences a default at an unpredictable time τ , which follows a known risk-neutral distribution $Q(t) = \mathbb{Q}[\tau \leq t]$. Let $V_i(t)$ represent the value at time t of the i^{th} derivative from the institution’s perspective. The exposure refers to the value of all derivative contracts the institution has with the counterparty, which could incur a loss if the counterparty defaults before the maturity T (this corresponds to the maturity date of the portfolio’s longest contract). At any given time t , the exposure $E(t)$ is determined by the discounted values of all trades with the counterparty, represented by the set $\{\mathbf{V}_i(t)\}_{i=1}^N$. The total value of the counterparty’s portfolio at time t is expressed as $\mathbf{V}(t) = \sum_{i=1}^N \mathbf{V}_i(t)$. If netting is permitted, the exposure $E(t)$ is given by

$$E(t) = \max\{\mathbf{V}(t), 0\}. \tag{1}$$

Margin agreement defines the conditions under which margin (or collateral) must be posted to cover potential losses due to changes in the value of financial instruments such as derivatives. These agreements specify the types of acceptable collateral, the margin calculation methods, procedures for margin calls, and mechanisms for resolving disputes [35]. Margin requirements can vary depending on factors such as counterparty creditworthiness, asset volatility, and regulatory requirements. If the netting agreement is also supported by a margin agreement, the counterparty is required to provide collateral $C(t)$ to the bank, and the exposure is then given by

$$E(t) = \max\{\mathbf{V}(t) - C(t), 0\}. \tag{2}$$

Credit exposure becomes relevant only in the event of a counterparty default. Therefore, exposure assessments are contingent on this occurrence. In the following discussion, we focus on exposure calculations without considering default events, implicitly assuming no “wrong-way risk” is present. The expected exposure (EE) represents the expected value, conditioned on the mark-to-market (MtM) of the derivatives portfolio being positive. It reflects the average of the positive MtM values in the future, discounted to the present using the risk-free rate [14]. ($D(t, u) = \exp(-\int_t^u r_s ds)$, where (r_s) represents the instantaneous risk-free short rate process). Under the risk-neutral measure, it is given by

$$EE(t, u) = \mathbb{E}^Q[D(t, u)E(u)]. \tag{3}$$

As discussed in the next section, the expected exposure (EE) plays a central role in the calculation of the credit valuation adjustment.

2.2. Credit Valuation Adjustment (CVA)

The credit valuation adjustment (CVA) plays a crucial role for financial institutions in evaluating and mitigating counterparty credit risk, especially in the context of derivative trading where the exposures are often considerable. It allows banks to price derivative transactions correctly and allocate capital efficiently. By definition, CVA represents the difference between the value of a derivative portfolio in a risk-free scenario and its actual value that incorporates the possibility of counterparty default. Typically, CVA is calculated as the present value of expected losses arising from a counterparty’s default, discounted at the risk-free rate. This calculation involves modeling the default probability of the counterparty, the loss given default (LGD), and the exposure at default (EAD). Assuming no wrong-way risk and deterministic survival probabilities $S(.,.)$, the CVA is expressed as follows [2,14,20,34,36]:

$$\begin{aligned} CVA(t, T) &= \mathbb{E}^Q\left[(1 - \mathbf{R})D(t, \tau)E(\tau) \times 1_{\{t \leq \tau \leq T\}}\right] \\ &= (1 - \mathbf{R}) \int_t^T \mathbb{E}^Q[D(t, u)E(u)]dS(t, u). \end{aligned} \tag{4}$$

The formula (4) can be computed using the following integration scheme:

$$\text{CVA}(t, T) = (1 - \mathbf{R}) \sum_{i=1}^m \text{EE}(t, t_i) [S(t, t_{i-1}) - S(t, t_i)]. \tag{5}$$

where the time periods are denoted as $t = t_0, t_1, t_2, \dots, t_m = T$. From this, we can see that the CVA depends on the following components:

- *Probability of Default (PD)*: For a nonconstant default intensity μ , the default probability and survival probability are given by

$$P(t, u) = 1 - S(t, u) = 1 - \exp \left[- \int_t^u \mu(x) dx \right]. \tag{6}$$

- *Loss Given Default (LGD)*: This is the portion of the exposure that is unrecoverable in the event of default. It quantifies the magnitude of losses in the event of default and is calculated as $1 - \mathbf{R}$, where \mathbf{R} is the recovery rate.
- *Exposure at Default (EAD)*: The expected exposure to the counterparty at the time of default τ is represented by $\text{EE}(t, \tau)$.

CVA is influenced by various factors such as the counterparty’s creditworthiness, market conditions, volatility of the underlying assets, and the maturity of the financial instruments involved.

3. Bayesian Inference Modeling

This section provides an overview of numerical integration through the lens of Bayesian inference. To ensure a comprehensive and precise presentation of Gaussian processes, numerical integration, and Bayesian quadrature, this discussion draws on insights and methodologies from references [31,37–40]. We begin by presenting the foundational tools necessary to understand the basic algorithm for probabilistic integration. Next, we tackle the problem of evaluating the integral of a function $f : \mathcal{X} \rightarrow \mathbb{R}$ over a domain $\mathcal{X} \subset \mathbb{R}^d$ with respect to a measure p on \mathcal{X} :

$$\mathcal{I} = \int_{\mathcal{X}} f(x) dp(x). \tag{7}$$

If a closed-form solution for this integral does not exist, numerical methods are required. These methods approximate the integral (7) using a weighted sum of function evaluations, which is known as a quadrature rule [38,39]:

$$\mathcal{Q}(f, \mathbf{X}, \omega) = \sum_{i=1}^N \omega_i f(x_i) = \omega^\perp f_{\mathbf{X}}, \tag{8}$$

where $\omega = [\omega_1, \dots, \omega_N] \in \mathbb{R}^N$ represents the real-valued weights, and $f_{\mathbf{X}} = [f(x_1), \dots, f(x_N)]^\perp \in \mathbb{R}^N$ denotes the function evaluations at the design points $\mathbf{X} = \{x_1, \dots, x_N\} \subset \mathcal{X}$. In essence, numerical integration aims to determine the optimal weights, design points, or both, to effectively compute (8).

3.1. Gaussian Process Regression

Gaussian processes [18,19,28,31,39,41] represent a sophisticated class of models that assign probability distributions to entire function classes. These models provide an effective framework for modeling and forecasting latent functions based on observed data. By taking advantage of the marginalization properties inherent in Gaussian processes, they enable flexible, nonparametric modeling, making them particularly well suited for Bayesian inference tasks, including regression and classification problems.

The Gaussian process (GP) is an extension of the normal distribution from a finite set of Gaussian random variables to an infinite collection [41]. As such, GPs are ideal for

representing random functions of the form $\mathbf{f} : \mathcal{X} \rightarrow \mathbb{R}$. The realizations of a GP are real-valued functions $f : \mathcal{X} \rightarrow \mathbb{R}$, where the values of f are considered a function of $x \in \mathcal{X}$ rather than just indices. More formally, let $\mathcal{X} \subset \mathbb{R}^d$ be a nonempty subset. A random process \mathbf{f} on $\mathcal{X} \subset \mathbb{R}^d$ is said to follow a Gaussian process $\mathbf{f} \sim \mathcal{GP}(m, k)$ with mean function $m : \mathcal{X} \rightarrow \mathbb{R}$ and covariance function $k : \mathcal{X} \times \mathcal{X} \rightarrow \mathbb{R}$ if, for any finite collection of points $\mathbf{X} = \{x_1, \dots, x_N\} \subset \mathcal{X}$ and any $N \in \mathbb{N}$, the vector $f_{\mathbf{X}} = [f(x_1), \dots, f(x_N)]^\top \in \mathbb{R}^N$ follows a multivariate normal distribution with

$$f_{\mathbf{X}} \sim \mathcal{N}(m(\mathbf{X}), K(\mathbf{X}, \mathbf{X})). \tag{9}$$

The mean vector is given by $[m(\mathbf{X})]_i = m(x_i)$ and the covariance matrix by $[K(\mathbf{X}, \mathbf{X})]_{ij} = k(x_i, x_j)$ for $i, j = 1, \dots, N$. The covariance function describes the covariance between the values of the function at two inputs, x and $x' \in \mathcal{X}$, and is defined as $k(x, x') = \mathbb{E}[(f(x) - m(x))(f(x') - m(x')))]$. The function $k(\cdot, \cdot)$, known as the kernel function, plays a central role in Gaussian process analysis. A widely used kernel in machine learning is the squared exponential kernel:

$$k(x, x') = \sigma_f^2 \exp\left(-\frac{(x - x')^2}{2l^2}\right). \tag{10}$$

where σ_f and l are non-negative scaling parameters. The covariance matrix $\mathbf{K} := K(\mathbf{X}, \mathbf{X})$ takes larger values when the points are closer and smaller values when they are farther apart. This behavior occurs because the points are more strongly correlated when their function values are similar and their variances are low, resulting in a higher covariance ([18]). The performance of Gaussian process regression (GPR) heavily relies on the choice of kernels, as they serve as a flexible prior for modeling functions in Bayesian inference tasks, such as regression and classification. GPR has been effectively applied to financial modeling, such as derivative portfolio analysis, and has proven its utility in CVA computations [1,18,19]. In GPR, the goal is to infer a latent function f from a finite set of observations, assuming that f is a sample path of an underlying Gaussian process $\mathbf{f} \sim \mathcal{GP}(m, k)$. Let us consider N data points $y = \{y_1, \dots, y_N\}$ at input locations $X = \{x_1, \dots, x_N\}$, summarized as the dataset $\mathcal{D} = \{X, y\}$, perturbed by independent and identically distributed Gaussian noise (Note that $y = f(x)$ in the absence of noise ($\sigma^2 = 0$). This corresponds to having noiseless observations of the latent function f):

$$y_i = f(x_i) + \epsilon_i, \quad \text{where } \epsilon_i \sim \mathcal{N}(0, \sigma^2). \tag{11}$$

The mean goal of Gaussian process regression is to compute the posterior $p(\mathbf{f} \mid \mathcal{D})$ and to predict function values at new input locations $x^* \in \mathcal{X}$. Specifically, the posterior is obtained using the conditioning rules for Gaussian processes, which require the joint probability distribution of the function values $\mathbf{f}^* := \mathbf{f}(x^*)$ at a new location x^* and the observed data y :

$$\begin{pmatrix} y \\ \mathbf{f}^* \end{pmatrix} \sim \mathcal{N}\left(\begin{pmatrix} m(X) \\ m(x^*) \end{pmatrix}, \begin{pmatrix} \mathbf{K} + \sigma^2 I_N & k(X, x^*) \\ k(X, x^*)^\top & k(x^*, x^*) \end{pmatrix}\right), \tag{12}$$

where $[k(X, x^*)]_i = k(x_i, x^*)$ is the covariance vector between the training points X and the new point x^* . We are interested in the conditional law $p(\mathbf{f}^* \mid \mathcal{D})$, which represents the probability of a certain prediction for $f(x^*)$ given the observed data. Using Equation (12) and the standard properties of conditioning Gaussian processes [31], the conditional distribution of \mathbf{f}^* given \mathcal{D} is

$$\mathbf{f}^* \mid \mathcal{D} \sim \mathcal{N}(m_{\mathcal{D}}(x^*), k_{\mathcal{D}}(x^*, x^*)), \tag{13}$$

where the posterior mean $m_{\mathcal{D}}(x^*)$ is given by

$$m_{\mathcal{D}}(x^*) = m(x^*) + k(x^*, X)(\mathbf{K} + \sigma^2 I_N)^{-1}(y - m(X)), \tag{14}$$

and the posterior variance $k_{\mathcal{D}}(x^*, x^*)$ is

$$k_{\mathcal{D}}(x^*, x^*) = k(x^*, x^*) - k(x^*, X)(\mathbf{K} + \sigma^2 I_N)^{-1}k(X, x^*). \tag{15}$$

If the prior mean m is assumed to be zero, the posterior mean $\mathbb{E}[\mathbf{f}^* \mid \mathcal{D}]$ can be expressed as

$$\mathbb{E}[\mathbf{f}^* \mid \mathcal{D}] = \sum_{i=1}^N \omega_i k(x_i, x^*), \quad \text{where } \omega = (\mathbf{K} + \sigma^2 I_N)^{-1}y. \tag{16}$$

The formula (16) allows the posterior mean to be computed without explicitly inverting $\mathbf{K} + \sigma^2 I_N$ by solving $(\mathbf{K} + \sigma^2 I_N)\omega = y$. Alternatively, grouping terms $k(x^*, X)^\top (\mathbf{K} + \sigma^2 I_N)^{-1}$, the posterior mean can also be written as

$$\mathbb{E}[\mathbf{f}^* \mid \mathcal{D}] = \sum_{i=1}^N \phi_i y_i, \quad \text{where } \phi = k(x^*, X)^\top (\mathbf{K} + \sigma^2 I_N)^{-1}. \tag{17}$$

3.2. Training Gaussian Process Algorithms

The practical application of Gaussian process regression relies heavily on the appropriate selection of the covariance function. This requires a careful determination of the kernel hyperparameters l and σ_f . Let $\theta = \{l, \sigma_f\}$ represent the model parameters. The standard approach to selecting these hyperparameters involves maximizing the log marginal likelihood $l(\theta) = \ln(p(y \mid \theta))$ [41], expressed as

$$l(\theta) = \ln(p(y \mid \theta)) = -\frac{1}{2}y^\top (\mathbf{K} + \sigma^2 I_n)^{-1}y - \frac{1}{2} \ln(|\mathbf{K} + \sigma^2 I_n|) - \frac{n}{2} \ln(2\pi), \tag{18}$$

where the first term in Equation (18) quantifies data fit, the second term represents a complexity penalty, and the last term serves as a normalization constant. Assuming a zero-mean prior and noiseless observations, the partial derivatives of the log marginal likelihood with respect to the hyperparameters are given by

$$\begin{aligned} \frac{\partial l(\theta)}{\partial \theta_j} &= \frac{1}{2}y^\top \mathbf{K}^{-1} \frac{\partial \mathbf{K}}{\partial \theta_j} \mathbf{K}^{-1}y - \frac{1}{2} \text{tr} \left(\mathbf{K}^{-1} \frac{\partial \mathbf{K}}{\partial \theta_j} \right) \\ &= \frac{1}{2} \text{tr} \left(\omega \omega^\top - \mathbf{K}^{-1} \frac{\partial \mathbf{K}}{\partial \theta_j} \right), \end{aligned} \tag{19}$$

where $\omega = \mathbf{K}^{-1}y$. One significant limitation of Gaussian processes is their poor scalability with the number of observations n . The computational complexity of evaluating the marginal likelihood in Equation (18) is primarily dictated by the inversion of the covariance matrix \mathbf{K} . The log determinant of \mathbf{K} is computed as a by-product of the matrix inversion. For symmetric positive definite matrices of size $n \times n$, standard matrix inversion methods require $\mathcal{O}(n^3)$ time. Once \mathbf{K}^{-1} is available, the derivatives in Equation (19) can be calculated in $\mathcal{O}(n^2)$ time per hyperparameter. Consequently, the cost of derivative computation is relatively small, enabling the optimization problem in Equation (18) to be efficiently addressed using techniques such as gradient descent, conjugate gradient, or quasi-Newton algorithms.

3.3. Bayesian Quadrature

With Gaussian process regression established as a modeling tool, we can now revisit the intractable integral in (7). Bayesian quadrature [37–40] offers a probabilistic framework for approximating such integrals by modeling the target function f as a Gaussian process.

This approach replaces the deterministic function f with a stochastic process \mathbf{f} , transforming the numerical integration problem (7) into a random variable \mathbf{I} , defined as

$$\mathbf{I} = \int_{\mathcal{X}} \mathbf{f}(x) dp(x). \tag{20}$$

As the integration operator is a linear functional, the integral of a Gaussian process also follows a Gaussian distribution. Thus, it is more natural to consider a prior distribution over the integrand rather than the integral itself, as quadrature rules (8) rely on pointwise evaluations $f(x_1), \dots, f(x_N)$. For specific kernel–prior combinations, the weights of the quadrature can be computed analytically.

Although maintaining the Gaussian process model requires computational resources, this approach generalizes the information obtained from samples across the integration domain. This enables the targeted selection of sample points, making Bayesian quadrature a competitive and efficient alternative to Monte Carlo methods.

Assuming a Gaussian process prior $\mathbf{f} \sim \mathcal{GP}(\mathbf{m}, k)$, the resulting prior over the integral \mathbf{I} is a univariate Gaussian distribution:

$$\mathbf{I} \sim \mathcal{N}(\mathbf{m}, \nu),$$

where

$$\mathbf{m} = \mathbb{E}_f[\mathbf{I}] = \int_{\mathcal{X}} m(x) dp(x), \quad \nu = \mathbb{V}_f[\mathbf{I}] = \iint_{\mathcal{X} \times \mathcal{X}} k(x, x') dp(x) dp(x'). \tag{21}$$

Given the data $\mathcal{D} = \{X, y\}$, comprising nodes and function evaluations, Gaussian Process Regression (GPR) can be employed on the posterior distribution $f | \mathcal{D}$ using the integral operator. Bayesian quadrature thus provides a systematic method for handling noisy observations y of the integrand f , as described in (11). The linearity of Gaussian processes allows us to express the joint distribution of (y, \mathbf{I}) as

$$\begin{pmatrix} y \\ \mathbf{I} \end{pmatrix} \sim \mathcal{N} \left(\begin{bmatrix} m(X) \\ \mathbf{m} \end{bmatrix}, \begin{bmatrix} \mathbf{K} + \sigma^2 I_N & \int_{\mathcal{X}} k(X, x) dp(x) \\ \int_{\mathcal{X}} k(x, X)^\top dp(x) & \iint_{\mathcal{X} \times \mathcal{X}} k(x, x') dp(x) dp(x') \end{bmatrix} \right). \tag{22}$$

Conditioning on the observed data y yields the posterior distribution $\mathbf{I} | y \sim \mathcal{N}(\mathbf{m}_{\mathcal{D}}, \nu_{\mathcal{D}})$, where the posterior mean $\mathbf{m}_{\mathcal{D}}$ is given by

$$\begin{aligned} \mathbf{m}_{\mathcal{D}} &= \mathbb{E}_{f|\mathcal{D}}[\mathbf{I}] \\ &= \int_{\mathcal{X}} \left[m(x) + k(x, X)^\top (\mathbf{K} + \sigma^2 I_N)^{-1} (y - m(X)) \right] dp(x) \\ &= \int_{\mathcal{X}} m(x) dp(x) + \sum_{i=1}^N \int_{\mathcal{X}} k(x, x_i) dp(x) \left[(\mathbf{K} + \sigma^2 I_N)^{-1} (y - m(X)) \right]_i, \end{aligned} \tag{23}$$

and the posterior variance $\nu_{\mathcal{D}}$ is given by

$$\begin{aligned} \nu_{\mathcal{D}} &= \mathbb{V}_{f|\mathcal{D}}[\mathbf{I}] \\ &= \iint_{\mathcal{X} \times \mathcal{X}} \left[k(x, x') - k(x, X)^\top (\mathbf{K} + \sigma^2 I_N)^{-1} k(X, x') \right] dp(x) dp(x') \\ &= \iint_{\mathcal{X} \times \mathcal{X}} k(x, x') dp(x) dp(x') \\ &\quad - \sum_{i,j=1}^N \left[(\mathbf{K} + \sigma^2 I_N)^{-1} \right]_{ij} \int_{\mathcal{X}} k(x, x_i) dp(x) \int_{\mathcal{X}} k(x_j, x') dp(x'). \end{aligned} \tag{24}$$

Implementing Bayesian quadrature numerically clearly requires the calculation of two essential integrals: the kernel mean $\kappa(x) = \int_{\mathcal{X}} k(x, x') dp(x')$ and the initial variance

$v = \iint_{\mathcal{X} \times \mathcal{X}} k(x, x') dp(x) dp(x')$. Denoting the vector of kernel means evaluated at nodes \mathbf{X} as $\kappa := \kappa(x)$, Equations (23) and (24) can be expressed more concisely as

$$\mathbf{m}_{\mathcal{D}} = \mathbf{m} + \kappa^{\top} (\mathbf{K} + \sigma^2 I_N)^{-1} (y - m(\mathbf{X})) \quad \text{and} \quad v_{\mathcal{D}} = v - \kappa^{\top} (\mathbf{K} + \sigma^2 I_N)^{-1} \kappa. \quad (25)$$

In the specific case of a zero prior mean and noise-free observations, the posterior mean of \mathbf{I} simplifies to

$$\mathbf{m}_{\mathcal{D}} = \kappa^{\top} \mathbf{K}^{-1} f = \sum_{i=1}^N \omega_i f(x_i), \quad \text{where} \quad \omega = \mathbf{K}^{-1} \kappa. \quad (26)$$

The formula (26) represents the standard version of a quadrature rule, Equation (8), which approximates the integral as a weighted sum of the function evaluations. Bayesian quadrature reformulates the integral (7) by substituting the integrals of the kernel function. To improve computational efficiency, the kernel used in Bayesian quadrature is typically chosen so that the kernel mean and initial variance can be derived analytically. The process for numerically approximating the integral (7) using Bayesian quadrature is summarized in Algorithm 1.

Algorithm 1 Bayesian quadrature.

Input: $\mathcal{G}\mathcal{P}(m, k), p(\cdot), \mathcal{D} = \{\mathbf{X}, y\}, \sigma^2$

Output: Bayesian quadrature estimation of the integral \mathbf{I}

```

1: procedure BQ( $f(\cdot), \mathcal{G}\mathcal{P}(m, k), p(\cdot), \mathcal{D}, \sigma^2$ )
2:    $\kappa \leftarrow \int_{\mathcal{X}} k(\mathbf{X}, x) dp(x)$  // Compute kernel mean
3:    $v \leftarrow \iint_{\mathcal{X} \times \mathcal{X}} k(x, x') dp(x) dp(x')$  // Compute kernel variance
4:    $\mathbf{m} \leftarrow \int_{\mathcal{X}} m(x) dp(x)$  // Integrate prior mean
5:    $\mathbf{m} \leftarrow m(\mathbf{X})$ 
6:    $\omega \leftarrow (\mathbf{K} + \sigma^2 I_n)^{-1} \kappa$  // Compute quadrature weights
7:    $\mathbf{m}_{\mathcal{D}} \leftarrow \mathbf{m} + \omega^{\top} (y - \mathbf{m})$  // Compute Bayesian quadrature mean
8:    $v_{\mathcal{D}} \leftarrow v - \omega^{\top} \kappa$  // Compute kernel variance
9:    $p(\mathbf{I} | y) \leftarrow \mathcal{N}(\mathbf{m}_{\mathcal{D}}, v_{\mathcal{D}})$ 
10:  return  $p(\mathbf{I} | y)$ 
11: end procedure

```

4. CVA Calculation Under One-Factor Linear Gauss Markov

Calculating counterparty risk metrics and the CVA of a trading portfolio is commonly performed using Monte Carlo simulations, as this approach is generally straightforward to implement. The main drawback of this approach is its performance, as accuracy increases with the number of simulations. However, when adopting a specific modeling framework such as One-Factor Linear Gaussian Markov (LGM-1F), other alternative methods can serve as serious options for calculating these risk indicators, offering performance that compares very favorably to the Monte Carlo method. As mentioned earlier, the choice of the LGM-1F model was motivated by its status as the market consensus for valuing the majority of interest rate derivatives. Therefore, it seemed appropriate to use the same model to estimate the valuation adjustment for counterparty risk (CVA). Below, the derivative products comprising our trading portfolio are interest rate swaps and swaptions. Within this framework and alongside the Monte Carlo method, we present the numerical integration method for calculating the CVA of a portfolio of swaps and/or swaptions, as well as an analytical formula, used as a proxy, as reference methods for calculating the CVA of a portfolio of interest rate swaps.

Throughout the remainder of this paper, the LGM-1F model is used within a single-curve framework. However, it is important to note that our approach can also be applied within a multicurve framework for pricing and risk management of interest rate derivatives. The results of our study are independent of this choice.

In the LGM-1F framework [13,42,43], the dynamics of the zero-coupon bond $B(t, T)$ of maturity T is a lognormal process under risk-neutral probability \mathbb{Q} . In this case, the volatility of the zero-coupon bond is deterministic, and it is given by $\Gamma(t, T) = \frac{\sigma}{\lambda}(\exp(-\lambda(T-t)) - 1)$, where σ is a piecewise constant, and λ is a mean reversion constant. The LGM-1F assumption for interest rate modeling, derived from the HJM framework, is simple and tractable. The dynamics of the yield curve are specified by the piecewise constant short-term volatility σ and the mean reversion parameter λ , and it is given as follows:

$$dX_t = [\phi(t) - \lambda X_t]dt + \sigma(t)dW_t^{\mathbb{Q}}, \tag{27}$$

where

$$X_0 = 0 \quad \text{and} \quad \phi(t) = \int_0^t \sigma(s)^2 e^{-2\lambda(t-s)} ds. \tag{28}$$

Note that at any future date t , all zero-coupon bonds are obtained as deterministic functions of the state variable X_t . This deterministic relation is referred to as the construction formula, which is given as follows:

$$B(t, T) = \frac{B(0, T)}{B(0, t)} \exp\left(-\frac{1}{2}\beta(t, T)^2\phi(t) - \beta(t, T)X_t\right) \quad \text{and} \quad \beta(t, T) = \frac{1 - \exp(-\lambda(T-t))}{\lambda}. \tag{29}$$

Let us Consider an interest rate swap, and let $T_0 < T_1 < \dots < T_n$ denote the settlement dates for the fixed leg (no flows exchanged in T_0). The fixed swap rate defined at date t ($t \leq T_0$) equals

$$S(t, T_0, T_n) = \frac{B(t, T_0) - B(t, T_n)}{LVL(t, T_0, T_n)} \quad \text{where} \quad LVL(t, T_0, T_n) = \sum_{i=1}^n \delta_i B(t, T_i). \tag{30}$$

The parameter δ_i is the year fraction between T_{i-1} and T_i calculated in the adequate basis. In this setup, the value of a payer fixed coupon interest rate swap with rate K (the strike of the swap rate) at a future date t can be expressed as follows:

$$V(t, X_t) = B(t, T_0) - B(t, T_n) - K \times \sum_{i=1}^n \delta_i B(t, T_i). \tag{31}$$

The calculation of the expected exposure $\mathbf{EE}(t)$ at a future date t for a portfolio of interest rate swaps under this framework can be calculated either by Monte Carlo simulations or through a one-dimensional integral involving portfolio value $V(t, \cdot)$ function and the density ϕ_t of the Gaussian variable X_t under the terminal probability measure \mathbb{Q}_t as follows (We adopt the notation $x^+ := \max(x, 0)$ for any real number x):

$$\begin{aligned} \mathbf{EE}(t) &= \mathbb{E}^{\mathbb{Q}}[D(0, t) V(t, X_t)^+] \\ &= B(0, t) \mathbb{E}^{\mathbb{Q}_t}[V(t, X_t)^+] \\ &= B(0, t) \int_{-\infty}^{+\infty} V(t, x)^+ \phi_t(x) dx. \end{aligned} \tag{32}$$

We refer the reader to Appendix A for more details on the change of measure.) In the following, the CVA of the interest rate swaps portfolio is given by

$$\begin{aligned} \mathbf{CVA} &= (1 - R) \times \mathbb{E}^{\mathbb{Q}}\left[B(0, \tau) \times \left(\int_{-\infty}^{+\infty} V(\tau, x)^+ \phi_{\tau}(x) dx\right) \times 1_{\tau \leq T_e}\right] \\ &= (1 - R) \int_0^T \int_{-\infty}^{+\infty} B(0, t) V(t, x)^+ \phi_t(x) dx dS(0, t). \end{aligned} \tag{33}$$

The computation of the expected exposure using Formula (32) is referred to as the numerical integration method (NI method) in this paper.

4.1. Analytical CVA Approximation Under LGM-1F Model

It can also be practical at times to quickly estimate the expected exposure and CVA of an interest rate swap portfolio, or the marginal contribution of a swap to such a portfolio, outside the official simulation system. To achieve this, we demonstrate that the value distribution of such a portfolio under LGM-1F can be approximated by a Gaussian distribution. We consider a portfolio of n interest rate swaps, where the value of each swap at a future date t is denoted by $V_i(t)$ for $i = 1, 2, \dots, n$. Without loss of generality, if we consider the swaps with values V_i as payers, we can express $V_i(t)$ as follows:

$$V_i(t) = \sum_{k=0}^{m_i} c_k^i B(t, T_k^i), \tag{34}$$

where

$$c_0^i = 1, \quad c_{m_i}^i = 1 - (T_{m_i}^i - T_{m_i-1}^i)K_i, \quad c_k^i = -(T_k^i - T_{k-1}^i)K_i \quad k = 1, \dots, m_i - 1. \tag{35}$$

By performing a first-order Taylor expansion of $B(t, T_k^i)$ from Formula (??) with respect to X_t , we obtain the following approximation:

$$B(t, T_k^i) \approx A(t, T_k^i) - A(t, T_k^i)\beta(t, T_k^i)X_t, \tag{36}$$

where

$$A(t, T_k^i) = \frac{B(0, T_k^i)}{B(0, t)} \times \exp\left(-\frac{1}{2}\beta(t, T_k^i)^2\phi(t)\right). \tag{37}$$

Taking this approximation into account, the future value $V_i(t)$ of swap i for $i = 1, 2, \dots, n$ in the portfolio is normally distributed and can be estimated as an affine function of the Gaussian variable X_t , which characterizes the dynamics of the LGM-1F:

$$V_i(t) \approx \left[\sum_{k=0}^{m_i} c_k^i A(t, T_k^i) \right] - \left[\sum_{k=0}^{m_i} c_k^i A(t, T_k^i)\beta(t, T_k^i) \right] X_t. \tag{38}$$

As the sum of normal variables remains normal, the portfolio value $V(t) = \sum_{i=1}^n V_i(t)$ is normally distributed, and it is expressed as an affine function of the Gaussian variable X_t

$$V(t) \approx \left[\sum_{i=1}^n \sum_{k=0}^{m_i} c_k^i A(t, T_k^i) \right] - \left[\sum_{i=1}^n \sum_{k=0}^{m_i} c_k^i A(t, T_k^i)\beta(t, T_k^i) \right] X_t. \tag{39}$$

The expected value and the standard deviation of the portfolio value $V(t)$ at any future time t are given by

$$\mu_P(t) = \left[\sum_{i=1}^n \sum_{k=0}^{m_i} c_k^i A(t, T_k^i) \right] - \left[\sum_{i=1}^n \sum_{k=0}^{m_i} c_k^i A(t, T_k^i)\beta(t, T_k^i) \right] \mathbb{E}(X_t). \tag{40}$$

and

$$\sigma_P^2(t) = \left[\sum_{i=1}^n \sum_{k=0}^{m_i} c_k^i A(t, T_k^i)\beta(t, T_k^i) \right]^2 \times \mathbb{V}(X_t). \tag{41}$$

Therefore, the expected exposure $\mathbb{E}\mathbb{E}(t)$ of the interest rate swaps portfolio is given by

$$\begin{aligned} \mathbb{E}\mathbb{E}(t) &= B(0, t) \mathbb{E}^{\mathbb{Q}_t} [\max(\mu_P(t) + \sigma_P(t)Z, 0)] \\ &= B(0, t) \int_{-\frac{\mu_P(t)}{\sigma_P(t)}}^{+\infty} (\mu_P(t) + \sigma_P(t)x) \Phi(x) dx \\ &= B(0, t) \left[\mu_P(t) N\left(\frac{\mu_P(t)}{\sigma_P(t)}\right) + \sigma_P(t) \Phi\left(\frac{\mu_P(t)}{\sigma_P(t)}\right) \right]. \end{aligned} \tag{42}$$

where Φ is the probability density function of the standard normal distribution, and N corresponds to its cumulative distribution function. The actual calculation of the mean $\mu_P(t)$ and standard deviation $\sigma_P(t)$ of the interest rate swap portfolio is based on the mean and standard deviation of the variable X_t . In the context of the LGM-1F model, the integrated form of the dynamics of X_t is given as follows:

$$X_t = \int_0^t \phi(s)e^{-\lambda(t-s)} ds + \int_0^t \sigma(s)e^{-\lambda(t-s)} dW_s^{\mathbb{Q}} \tag{43}$$

$$= \int_0^t (\phi(s) + \sigma(s)\Gamma(s, t))e^{-\lambda(t-s)} ds + \int_0^t \sigma(s)e^{-\lambda(t-s)} dW_s^{\mathbb{Q}_t}. \tag{44}$$

So, the mean and standard deviation—under \mathbb{Q}_t —can be obtained analytically as follows:

$$\mathbb{E}(X_t) = \int_0^t (\phi(s) + \sigma(s)\Gamma(s, t))e^{-\lambda(t-s)} ds \quad \mathbb{V}(X_t) = \int_0^t \sigma(s)^2 e^{-2\lambda(t-s)} ds \tag{45}$$

The Credit Valuation Adjustment is assessed at the counterparty level, but there are instances where it is beneficial to identify the contributions of individual trades to the counterparty-level CVA. This can be straightforwardly achieved using an analytical formula when the exposure distribution is Gaussian, as it is in this context. For further details on this topic, refer to ([34]).

4.2. Swaption Valuation with LGM-1F Model

Consider a swap with expiry date T_e . Let $T_0 < T_1 < \dots < T_n$ (with $T_e < T_0$) denote the settlement dates or the fixed leg (no flows exchanged in T_0). The fixed swap rate defined at date T_e equals

$$S(T_e, T_0, T_n) = \frac{B(T_e, T_0) - B(T_e, T_n)}{LVL(T_e, T_0, T_n)} \quad \text{where} \quad LVL(T_e, T_0, T_n) = \sum_{i=1}^n \delta_i B(T_e, T_i). \tag{46}$$

The parameter δ_i represents the year fraction between T_{i-1} and T_i calculated in the adequate basis. A payer swaption of strike K written on the above swap is an option maturing in T_e with payoff

$$LVL(T_e, T_0, T_n)(S(T_e, T_0, T_n) - K)^+ = \left(B(T_e, T_0) - B(T_e, T_n) - \sum_{i=1}^n \delta_i K B(T_e, T_i) \right)^+ \tag{47}$$

Within the framework of the LGM-1F, it can be demonstrated that the payoff of the swaption can be expressed as a weighted sum of call options with appropriately chosen underlyings and strike prices:

$$LVL(T_e, T_0, T_n)(S(T_e, T_0, T_n) - K)^+ = \sum_{i=1}^n c_i \left(\frac{B(T_e, T_i)}{B(T_e, T_0)} - K_i \right)^+, \tag{48}$$

where $c_i = \delta_i K$ for $i = 1, \dots, n - 1$, $c_n = 1 + \delta_n K$ and $K_i = \frac{B_{T_e, T_i}(x_0)}{B_{T_e, T_0}(x_0)}$. (If we write $B(T_e, T_i) = B_{T_e, T_i}(X_{T_e})$, we can see from Equation (??) that , for all i , $x \rightarrow \sum_{i=1}^n c_i \frac{B_{T_e, T_i}(x)}{B_{T_e, T_0}(x)}$ is strictly decreasing, so that it is a bijection between \mathbb{R} and $]0, +\infty[$. As a consequence, there exists a

unique $x_0 \in \mathbb{R}$ such that $\sum_{i=1}^n c_i \frac{B_{T_e, T_i}(x_0)}{B_{T_e, T_0}(x_0)} = 1$. By construction, the n call options in (39) all have the same exercise domain—defined by $X_{T_e} < x_0$ —as the payer swaption.) According to Black–Scholes theory, the price of a swaption in date $t = 0$ can be expressed as follows:

$$\begin{aligned} V^*(0, T_e, T_0, T_n) &= B(0, T_e) \times \mathbb{E}^{\mathbb{Q}^{T_e}} \left[\left(B(T_e, T_0) - B(T_e, T_n) - \sum_{i=1}^n \delta_i K B(T_e, T_i) \right)^+ \right] \\ &= B(0, T_0) \times \sum_{i=1}^n c_i \times P_i^{bs}(F_i, 0, \sigma_i^{bs}, K_i, T_e). \end{aligned} \tag{49}$$

where P_i^{bs} denotes the Black and Scholes price of a call option, and F_i and σ_i^{bs} are given as follows:

$$F_i = \frac{B(0, T_i)}{B(0, T_e)} \quad \text{and} \quad \sigma_i^{bs} = \frac{1}{\sqrt{T_e}} \beta(T_e, T_i) \sqrt{\phi(T_e)}. \tag{50}$$

The pricing formula for European swaptions is quasiclosed because the calculation of the strikes K_i for $i = 1, \dots, n$ requires numerically solving the zeros of a nonlinear function. This can be time-consuming if this formula is used repeatedly, such as in the case of calculating the CVA of a trading portfolio including swaptions through Monte Carlo simulations. To overcome this limitation, we propose in the next subsection a fast approximation to price European swaptions under the LGM-1F model.

4.3. Swaption Valuation with Bachelier Model

In the following, we propose an alternative method for pricing a swaption based on an approximation of the dynamics of the swap rate within the framework of the LGM-1F. To achieve this, we seek to calculate the differential $dS(t)$ using Formula (30) by applying Itô’s lemma and neglecting the terms present in the drift (for simplicity of notations, we omit the dependence to T_0 and T_n in the swap rate: $S(t) := S(t, T_0, T_n)$):

$$dS(t) = \left[\frac{dB(t, T_0) - dB(t, T_n)}{\sum_{i=1}^n \delta_i B(t, T_i)} - \frac{B(t, T_0) - B(t, T_n)}{(\sum_{i=1}^n \delta_i B(t, T_i))^2} \sum_{i=1}^n \delta_i dB(t, T_i) \right] + (\dots)dt. \tag{51}$$

Using the assumptions made about the dynamics of the zero-coupon rates within the framework of the LGM-1F, we obtain the following expression for $\lambda \neq 0$:

$$dS(t) = \frac{\sigma(t)}{\lambda} e^{\lambda t} S(t) \left(\frac{B(t, T_0)e^{-\lambda T_0} - B(t, T_n)e^{-\lambda T_n}}{B(t, T_0) - B(t, T_n)} - \frac{\sum_{i=1}^n \delta_i B(t, T_i)e^{-\lambda T_i}}{\sum_{i=1}^n \delta_i B(t, T_i)} \right) dW_t^{\mathbb{Q}} + (\dots)dt. \tag{52}$$

In order to simplify the notation, we introduce a function $g(\cdot)$ such that

$$dS(t) = \sigma(t) e^{\lambda t} g(t) S(t) dW_t^{\mathbb{Q}} + (\dots)dt. \tag{53}$$

Equation (53) suggests adopting one of the following two approximations:

- Assuming log-normal dynamics for the swap rate with a frozen g .
- Assuming Gaussian dynamics for the swap rate with a frozen drift.

To obtain the Gaussian approximation, we set aside the drift term and then freeze the expression of function $g(t)S(t)$ at its initial value, i.e., $\forall t > 0, g(t)S(t) \approx g(0)S(0)$. We thus obtain the approximation of the normal dynamics of the interest rate $S(t)$:

$$dS(t) = \sigma(t) e^{\lambda t} g(0) S(0) dW_t^{\mathbb{Q}}. \tag{54}$$

We conducted a comparative study between the empirical LGM-1F distribution of the swap rate and the underlying Gaussian and log-normal distributions of the two approximations.

The numerical tests reveal that the swap rate distribution is closer to Gaussian than log-normal. To illustrate this, the results of the comparative study are summarized in the Figure 1. In the following, we will only consider the case where $\lambda \neq 0$, but the equations and the function g can be adapted for $\lambda = 0$. One way to test the validity of the normality assumption of swap rates under the LGM-1F model used in the approximation is to compare the empirical distribution of a swap rate with the Gaussian distribution of swap rates at a given date t . To do this, we focus on the distribution of the swap rate at the date $t = 3Y$. This swap starts at $T_0 = 3Y$ and matures at $T_n = 10Y$. The payment frequency is semiannual. We used 30,000 simulations. The empirical distribution was constructed based on 30 homogeneous classes. In Figure 1, the histogram corresponds to the empirical distribution obtained through Monte Carlo simulations. The curve represents the theoretical Gaussian distribution of the approximation. The distribution tests show that the Gaussian approximation of the swap rate dynamics is very close to the dynamics obtained within the LGM-1F framework. The quality of the approximation is stable for different levels of instantaneous volatility σ and mean reversion λ . Therefore, the approximation seems more suitable for our modeling choice.

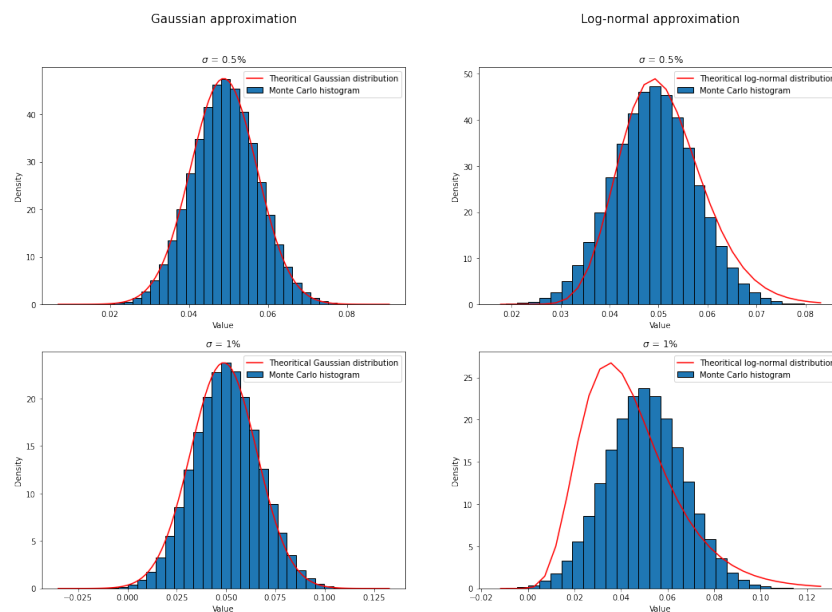


Figure 1. Comparison of the Gaussian approximation, the log-normal approximation, and the empirical distribution of a forward swap rate obtained with the LGM-1F model via Monte Carlo simulations. This comparison was performed for two different values of $\sigma \in \{0.5\%, 1\%\}$ and $\lambda = 1\%$.

Where the dynamics of the interest rate $S(t)$ are governed by the normal process (54), the price of a swaption can be obtained using the Bachelier formula as follows (For the change of measure, we refer the reader to Appendix A. Note that we neglect the drift term associated to this change in measure in the dynamic of the swap rate $S(t)$, and the validity of this approximation is confirmed by the numerical tests in Section 5.):

$$\begin{aligned}
 V^*(0) &= \mathbb{E}^{\mathbb{Q}} [D(0, T_e) LVL(T_e) (S(T_e) - K)^+] = LVL(0) \mathbb{E}^{\mathbb{Q}^{LVL}} [(S(T_e) - K)^+] \\
 &= LVL(0) \left[S(0)\sigma^* \sqrt{T_e} \Phi\left(\frac{K - S(0)}{S(0)\sigma^* \sqrt{T_e}}\right) + (S(0) - K) \left(1 - N\left(\frac{K - S(0)}{S(0)\sigma^* \sqrt{T_e}}\right)\right) \right], \tag{55}
 \end{aligned}$$

where $\sigma^* \triangleq \frac{\sigma g(0)}{\sqrt{(T_e)}} \sqrt{\frac{e^{2\lambda T} - 1}{2\lambda}}$. Within this framework, the expected exposure $\mathbf{EE}(t)$ of a unitary interest rate swap at future date t is simply the value of the swaption written on the above swap with maturity t :

$$\mathbf{EE}(t) = \mathbb{E}^{\mathbb{Q}} [D(0, t) V(t, X_t)^+] = V^*(t) \tag{56}$$

In fact, the expected exposure can be calculated exactly using the closed-form Formula (49) or through the approximation (55). So, the CVA of the interest rate swap is expressed as follows:

$$\text{CVA} = (1 - R) \sum_{i=1}^m [S(0, t_{i-1}) - S(0, t_i)] \times V^*(t_i). \tag{57}$$

The CVA for an interest rate swap is calculated using a closed-form formula but based on the valuation of m swaptions (which correspond approximately to $m = 2500$ swaption valuations for the calculation of the CVA of a 10-year swap, assuming a daily discretization step), which can quickly become very time-consuming.

Now, denote the value of a European swaption at future time t as $V^*(t, X_t)$. In this case, the credit valuation adjustment (CVA) can be rewritten as follows:

$$\begin{aligned} \text{CVA} &= \mathbb{E}^{\mathbb{Q}}[(1 - R) \times D(0, \tau) V^*(\tau, X_{\tau})^+ \times 1_{\tau \leq T_e}] \\ &= (1 - R) \times \mathbb{E}^{\mathbb{Q}}[D(0, \tau) V^*(\tau, X_{\tau})] \times \mathbb{E}^{\mathbb{Q}}[1_{\tau \leq T_e}] \end{aligned} \tag{58}$$

As the exposure of the long swaption position can never be negative, the credit valuation adjustment (CVA) can be rewritten as follows:

$$\text{CVA} = (1 - R) \times P(0, T_e) \times V^*(0). \tag{59}$$

If the exposure to the counterparty consists of a portfolio of long and short positions in swaptions, this can be negative and, consequently, a closed-form formula for calculating the CVA is no longer available, and its computation become challenging.

5. Numerical Applications for CVA Calculation

This section aims to numerically evaluate the precision and speed of Bayesian quadrature for computing the CVA in a derivatives portfolio. We focus on a single case study involving a portfolio of 400 interest rate swaps in a single currency. The Gaussian process regression (GPR) is trained on the portfolio’s residual maturity and a single risk factor, namely, the short-term interest rate X_t of the LGM one-factor model. Although we consider a single currency portfolio here, this approach can be easily generalized to a multicurrency portfolio. In this context, Monte Carlo simulations serve as the benchmark method for our comparative study of expected exposure (EE) and CVA calculations. Most CVA calculations are carried out at the netting set level using Monte Carlo simulations. The expected exposure can be evaluated at the portfolio level, but in this study, we focus, without loss of generality, on CVA calculation at the netting set level. For the Monte Carlo simulations, we simulated 60,000 trajectories of market risk factors over 500 time steps into the future. This resulted in 30,000,000 simulations, which we used as the reference for the Monte Carlo simulations.

For the numerical implementation, we used Python and relied on widely adopted libraries for simulation and modeling. Specifically, NumPy was used for generating the random samples in the Monte Carlo simulations, while GPy and Emukit were employed for Gaussian process regression and Bayesian quadrature, respectively. These libraries offered robust and efficient tools for the statistical and machine learning models required in this work.

The parameters and input data used in the numerical tests, such as the characteristics of the interest rate swaps portfolio, the LGM-1F model settings, and the configuration of the GPR and Bayesian quadrature methods, are detailed in Appendix B. This appendix provides a comprehensive specification of all numerical elements, ensuring reproducibility and transparency.

The figures presented in this section visually complement the numerical experiments, offering insights into the accuracy, computational efficiency, and applicability of the meth-

ods under investigation. Each figure serves a specific purpose in demonstrating the methodology and validating the results.

5.1. Convergence Tests for a Unitary Interest Rate Swap

Before outlining the method for calculating the expected exposure (EE) and counterparty valuation adjustment (CVA) for a portfolio of swaps, we first address the calculation for a single swap. This can be accurately calculated using the closed-form expression (49) or the Bachelier Formula (55) for the expected exposure (56). In this numerical test, we verified the convergence conditions of the Bayesian quadrature method when calculating both EE and CVA for a single swap.

The key insights unveiled by Figure 2 are as follows: Figure 2 illustrates the expected exposure (EE) profile of an 8-year tenor interest rate swap, computed using three methods: the quasi-closed Formula (49) under the LGM-1F model with daily discretization, Gaussian approximation (55), and Monte Carlo simulations. The Monte Carlo simulations were performed with 10,000 samples (left graph) and 60,000 samples (right graph). The figure highlights key insights into the convergence properties of the EE profiles. It demonstrates that the Gaussian approximation is valid, and that 60,000 simulations were sufficient to achieve convergence to the reference swaption prices (LGM-1F). Moving forward, the Gaussian assumption of swap rates and the Bachelier formula serve as benchmarks for swaption pricing.

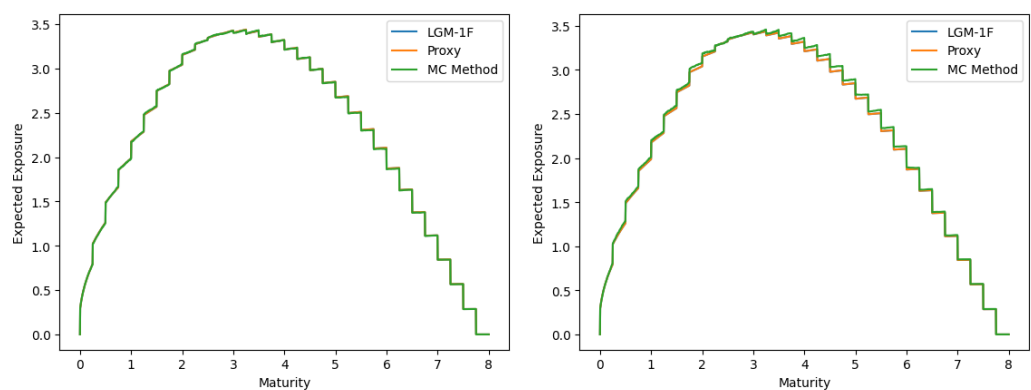


Figure 2. The expected exposure of an interest rate swap with a 8-year tenor and semiannual payments on both legs, calculated in three different ways (quasiclosed formula LGM-1F (49), closed formula based on the Gaussian approximation (55), Monte Carlo simulation pricing). (**left graph**) The Monte Carlo method uses 10,000 simulations, and (**right graph**) it uses 60,000 simulations.

Figure 3 depicts the expected exposure (EE) profile of an 8-year tenor interest rate swap, computed using the quasi-closed Formula (49) under the LGM-1F model with daily discretization and Gaussian process regression (GPR). The left panel utilizes 10 LGM-1F price observations, while the right panel is based on 20 observations. This analysis demonstrates that GPR provides an accurate fit to the EE profile with a limited number of training points, highlighting its computational efficiency and precision.

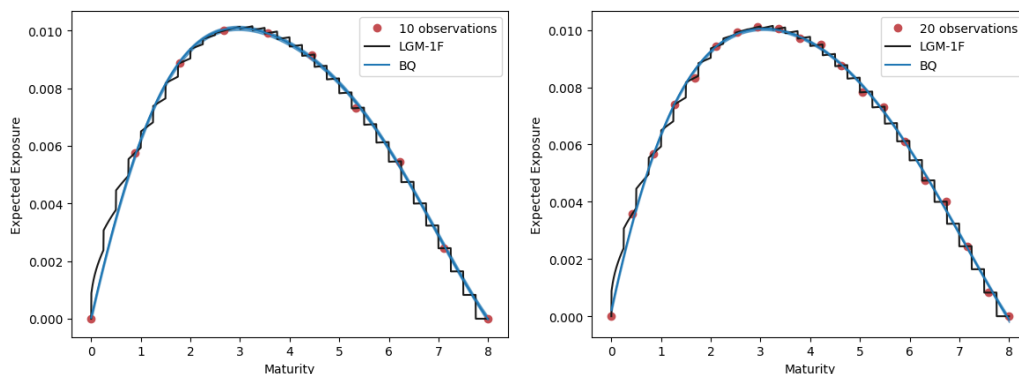


Figure 3. The expected exposure profile of an 8-year tenor interest rate swap, calculated directly using the quasiclosed Formula (49) under the LGM-1F model with daily discretization and with the Gaussian process regression (GPR) (the left figure uses 10 LGM-1F price observations, and the right figure uses 20 LGM-2F price observations).

5.2. CVA Calculation of an IRS Portfolio by Classical Approaches

We present a numerical example of an interest rate swap portfolio. The number of swaps was arbitrarily set at 400, with notional amounts uniformly set at EUR 10,000. Other swap characteristics, such as payment frequency and maturity, were randomly assigned. Without loss of generality, the valuation framework used was the single-curve approach. However, this did not affect our quantitative analysis, as our approach can be easily adapted to a multicurve framework. As a benchmark, we considered two approaches: (i) the full pricing by the Monte Carlo method combined with a numerical integration and (ii) two successive numerical integrations. More specifically, the expected exposure profile was computed either through the Monte Carlo method or via numerical integration (32). Subsequently, the CVA was determined through numerical integration with respect to the time to maturity.

Table 1 presents the CVA value computed using the Monte Carlo Method as a function of the number of simulations along with the corresponding computation times. Meanwhile, Table 2 displays the same results based on the number of discretizations. The numerical test highlighted that the Monte Carlo method converged at 60,000 simulations, yielding a CVA value of EUR 431 with a computation time of 33 min. In contrast, numerical integration achieved nearly the same value with a discretization step of 300, but with a computation time of only 40 s. It is important to note that in the example presented here, the implementation of the numerical integration is relatively straightforward. However, in the general case where the portfolio is influenced by multiple risk factors, this approach becomes more complex. As a result, the Monte Carlo method is typically the only viable option for effective numerical implementation, although it requires significant computational time. In this numerical example, the Gaussian proxy method described in Section 4.1, which relies on a quasianalytical formula for CVA calculation, can also be applied. Figure 4 illustrates the expected exposure profile for the interest rate swaps portfolio estimated using all three methods. Notably, the expected exposure profile calculated using the Gaussian proxy closely aligns with the profiles obtained from the other two methods.

Table 1. Calculation of CVA using Monte Carlo simulations.

No. of Simulations	CVA Value (EUR)	Computation Time (Seconds)
10,000	EUR 434	822
40,000	EUR 434	1053
60,000	EUR 431	2006
80,000	EUR 431	3165
100,000	EUR 431	9866

Table 2. Calculation of CVA using the numerical integration method.

Discretization Steps	CVA Value (EUR)	Computation Time (Seconds)
50	EUR 436	6
100	EUR 430	13
300	EUR 431	41
500	EUR 432	72
700	EUR 432	96

In Figure 4, the EE profile of a portfolio of 400 interest rate swaps is depicted, computed using three methods: Monte Carlo, numerical integration (NI), and the Gaussian proxy. The close alignment of the profiles across methods underscores the accuracy of the Gaussian proxy, particularly for low-volatility scenarios.

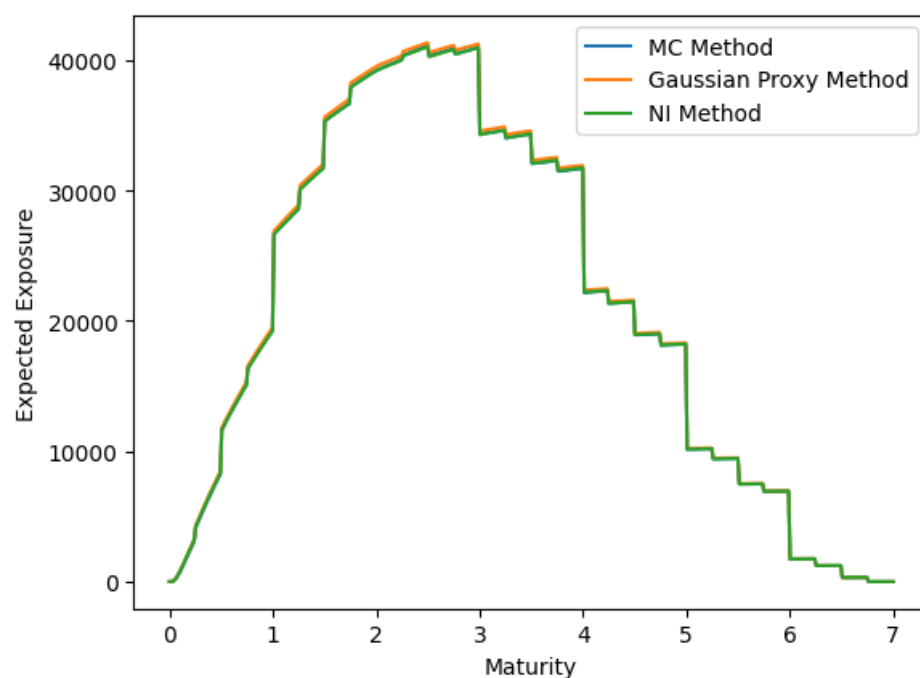


Figure 4. The expected exposure of a portfolio of 400 interest rate swaps computed with the Gaussian proxy, Monte Carlo, and NI methods.

Table 3 presents the numerical results of a comparative study between the Monte Carlo method, numerical integration (NI), and the Gaussian proxy. The proxy yields good results, particularly for relatively low volatility levels.

Table 3. Calculation of CVA using Gaussian proxy method.

LGM1F Volatility	MC Value (EUR)	NI Value (EUR)	Proxy Value (EUR)
0.5%	432	431	435
1%	629	628	642
1.5%	845	841	874
2%	1066	1062	1116

To ensure the robustness of the Gaussian approximation, we compared the density of the simulated value of an interest rate swaps portfolio at a future date with the densities obtained using the two other alternative methods for LGM1F volatility levels ranging between 50 and 200 basis points. The densities of the three methods are shown in Figure 5. This test demonstrates that the Gaussian proxy offers a good compromise between accuracy and computational time (13 s for the Gaussian proxy method, 72 s for the numerical integration method, and 33 min for the Monte Carlo method).

Regarding the key insights from Figure 5, this figure compares the density functions of portfolio values at a future date calculated using Monte Carlo, NI, and the Gaussian proxy for varying volatility levels. The results demonstrate that the Gaussian proxy offers a reasonable compromise between accuracy and computational speed, with computational times significantly lower than those of Monte Carlo.

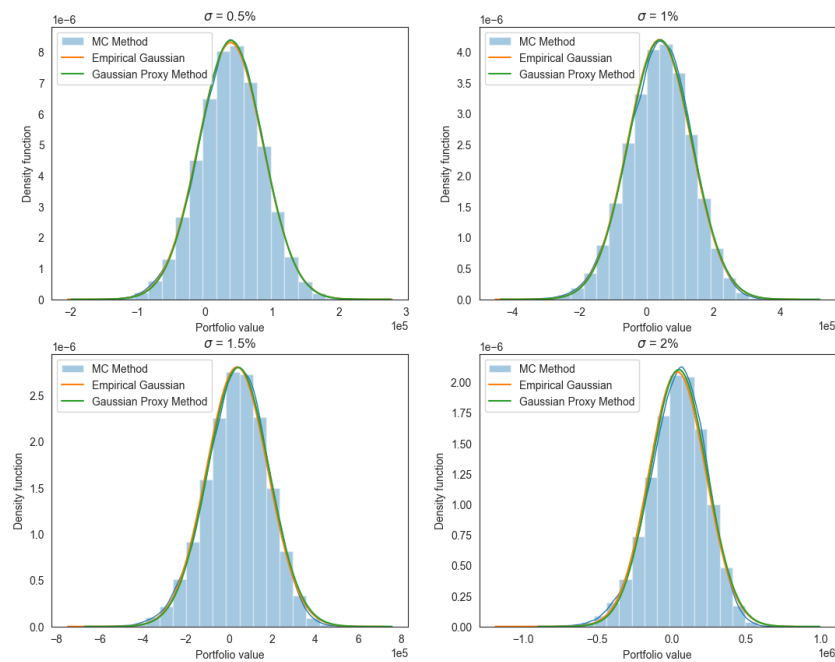


Figure 5. Comparison of density functions for interest rate swap portfolio simulation under LGM1F volatility.

5.3. Numerical Tests for CVA Calculation by GPR and Bayesian Quadrature

In this subsection, we revisit the previous numerical example of an interest rate swap portfolio to evaluate the performance of Bayesian quadrature in terms of accuracy and computational efficiency. As a benchmark, we compared it to the CVA calculation using the Monte Carlo method with 60,000 simulations and 500 time steps to compute the expected exposure profile across the portfolio’s maximum maturity. As explained earlier, Bayesian quadrature (BQ) and Gaussian process regression (GPR) training occurs along the time axis for numerical integration, as well as on the risk factors driving the portfolio, represented

here by the Gaussian variable X_t . Therefore, we conducted tests by varying the number of points used for training GPR and BQ.

The key insights from Figure 6 are as follows: The figure illustrates the portfolio values of 400 interest rate swaps at a future date computed using both a classical swap pricer and the GPR algorithm for 10,000 simulated values of the Gaussian variable X_t . This figure demonstrates the efficiency of GPR in estimating portfolio values with a limited number of training points. The results reveal that GPR achieves accurate approximations with as few as five training points, significantly reducing computational costs while maintaining precision.

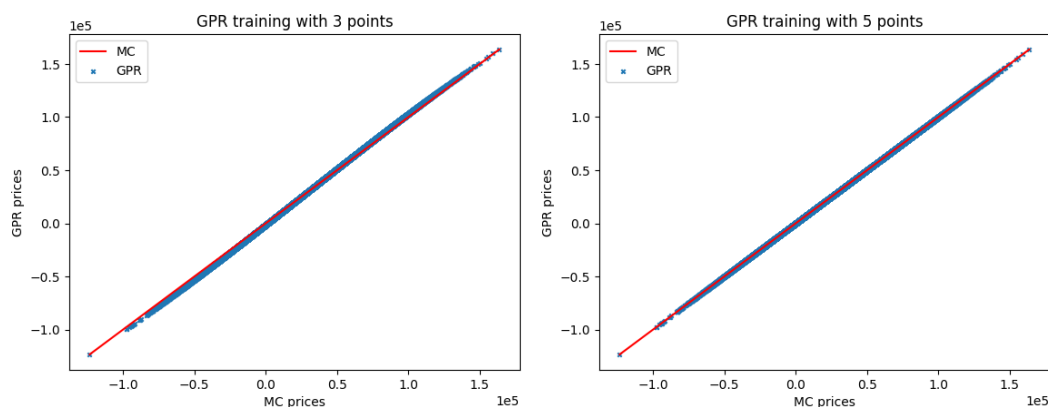


Figure 6. Comparison of Monte Carlo prices and GPR prices for 10,000 simulations on a given discretization date.

The calculation of the CVA and the expected exposure involves 60,000 simulations of the swap rate portfolio value at for 500 discretization dates. This process is time-consuming since each of the 400 swaps is individually valued for all 60,000 simulations. In the following numerical test, instead of calculating the portfolio value 60,000 times, we conducted it fewer times (e.g., 5 to 15 times). These valuations served as training points for the GPR. The above two graphs show that the GPR provides an excellent approximation with only five training points. Therefore, we selected five prices to train the GPR algorithm at each future date for the valuation of the portfolio's mark-to-market. Subsequently, these valuations were used to compute the expected exposures necessary for calculating the portfolio's CVA. Concurrently, we employed Bayesian quadrature, built upon Gaussian process regression, to compute the numerical integral underlying the CVA calculation. To achieve this, a very limited number of expected exposure computations were used to derive the entire expected exposure profile, which served as the cornerstone for CVA computation. Figure 7 displays the expected exposure profiles of the portfolio of 400 interest rate swaps for 15, 20, 30, and 40 observation points used in training the Bayesian quadrature algorithm.

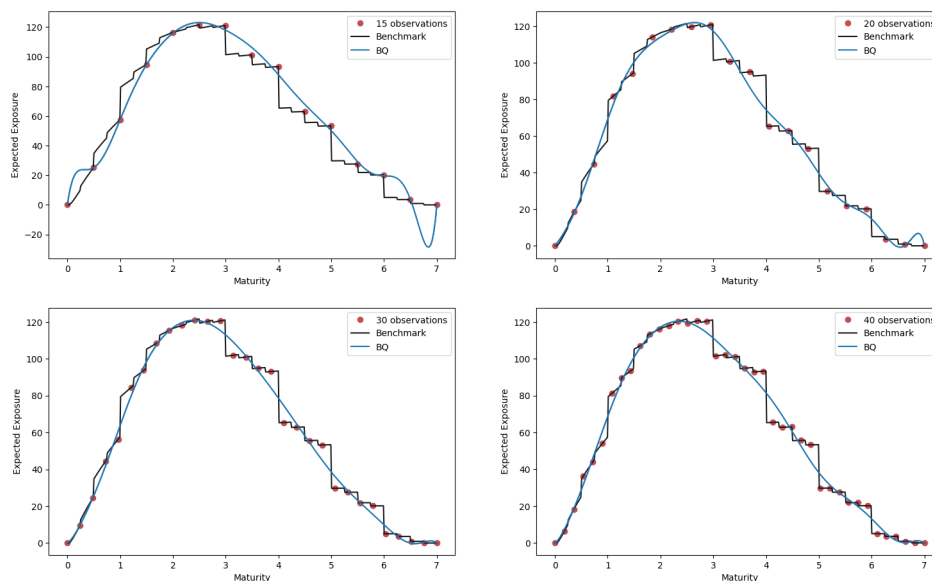


Figure 7. The expected exposure of the portfolio of 400 interest rate swaps for 4 different numbers of observations (15, 20, 30, and 40) used for training the Gaussian process.

The key insights from Figure 7 are as follows: This figure demonstrates the impact of varying the number of training observations (15, 20, 30, and 40) on the EE profiles of the swap portfolio using Bayesian quadrature. The results indicate that increasing the number of observations enhances accuracy, providing flexibility in balancing precision and computational efficiency.

The value of the interest rate swaps portfolio was estimated at EUR −54,507, with a corresponding CVA value of EUR 432. The execution time for the CVA calculation using Monte Carlo with 60,000 simulations was approximately 34 min (cf. Table 1).

Table 4. Calculation of CVA using the Bayesian quadrature method based on the number of training points, where the GPR is trained on time to maturity and X_t .

No. of Training Points	Bayesian Quadrature Prediction (EUR)	Relative Error	Computation Time (Seconds)	Time Savings
15	EUR 446	0.26	4	615
25	EUR 434	0.01	6	400
30	EUR 423	0.17	7	369
35	EUR 435	0.05	8	317
40	EUR 432	0.00	9	276

We conducted a numerical test using 40 training points for the GPR, with training currently performed on the time axis, and where the portfolio value was calculated using Gaussian process regression (trained with only five points) for the 60,000 simulations. The Bayesian quadrature method achieved a high level of accuracy while significantly reducing computation time to 9 s, compared to 31 min for Monte Carlo simulations. This indicates that under the conditions of this numerical test, the Bayesian quadrature method is 276 times faster than the Monte Carlo method while still ensuring a very high level of accuracy.

Remark 1. We conducted similar numerical tests, this time for a comparative study between traditional CVA calculation methods (numerical integration and Monte Carlo simulations) and

the Bayesian quadrature method for a portfolio of approximately one hundred swaptions. To achieve this, we used a proxy to value the swaptions with the Bachelier Formula (55), assuming that the forward swap rate followed a Gaussian distribution (54) within the LGM1F model. This approach significantly improved computation time compared to valuing swaptions using the LGM1F Formula (49). The numerical results confirmed that the Bayesian quadrature method outperformed traditional approaches (numerical integration method and Monte Carlo simulations) in terms of computation time while maintaining comparable accuracy.

6. Discussion

We are currently exploring new applications of Gaussian processes, specifically for market risk assessment. By combining Gaussian process regression (GPR) with multifidelity modeling, we aim to enhance the calculation of value at risk (VaR) and expected shortfall (ES) for complex portfolios, particularly those including Bermudan swaptions. These exotic derivatives present significant challenges for traditional risk measurement approaches, particularly in terms of computational costs. Multifidelity machine learning [44–48] combines data of varying levels of accuracy to develop precise models while reducing the need for high-fidelity data, which are often expensive or difficult to obtain. In our approach, we use low-fidelity pricing models to obtain general approximations and then refine the results with high-fidelity models, ensuring precision in risk metric calculations.

The preliminary results show that multifidelity Gaussian process regression (mGPR) provides substantial computational savings while maintaining high accuracy, especially for portfolios of Bermudan swaptions. This method reduces the computational costs associated with pricing these exotic derivatives while preserving the accuracy of risk measures like VaR and ES. We are currently preparing a detailed paper on this work, which will explore further improvements in this methodology, including optimizing point selection in multifidelity models. Additionally, we plan to extend this approach to other financial instruments and risk metrics with the goal of submitting this research in the near future.

7. Conclusions

In this study, we demonstrated the significant advantages of using Bayesian quadrature for the calculation of credit valuation adjustment (CVA) within the One-Factor Linear Gaussian Markov (LGM-1F) model framework. While traditional methods for CVA calculation are robust, they are often computationally intensive and time-consuming. Our research focused on applying Bayesian quadrature, a method based on Gaussian process regression (GPR), for CVA calculation, and compared it to traditional approaches. We found that Bayesian quadrature, with its exponential convergence and numerical stability, provides substantial reductions in computation time without sacrificing accuracy, making it a compelling alternative for real-time risk management.

The numerical results confirm that Bayesian quadrature not only outperforms traditional methods in terms of efficiency but also maintains comparable precision. This balance between speed and accuracy is critical for the practical implementation of CVA calculations, especially under increasingly stringent regulatory requirements. Furthermore, our application to a portfolio of fixed-income derivatives, including interest rate swaps and swaptions, within the LGM-1F model framework, highlights the versatility and robustness of Bayesian quadrature. This model is widely accepted for the valuation and risk management of such derivatives, making our findings highly relevant for financial institutions seeking to enhance their counterparty risk assessment processes.

The three main contributions of this study are as follows:

- An approximation of swaption prices using Bachelier's formula, which enables the modeling of forward-starting swap rates as Gaussian processes, facilitating efficient CVA computations,
- The proposal of an analytical approximation for the CVA of an interest rate swap portfolio, simplifying the calculation process while maintaining accuracy,

- The synergy between Gaussian process Regression and Bayesian quadrature, which optimizes numerical integration to achieve an innovative balance between computational efficiency and precision in credit risk management.

The integration of Bayesian quadrature and Gaussian processes also opens the door for further improvements. For instance, future research could explore optimizing point selection methods to further enhance computational efficiency and accuracy. Additionally, the adoption of a multifidelity approach [49] could combine models with varying levels of accuracy and computational cost, enabling more efficient resource use and improving the precision of CVA calculations.

In conclusion, Bayesian quadrature presents a powerful tool for the efficient and accurate calculation of CVA, offering a promising direction for future research and practical applications in financial risk management.

Author Contributions: Nouredine Lehdili contributed to the conceptualization, data curation, formal analysis, funding acquisition, investigation, methodology, project administration, resources, supervision, validation, visualization, and writing of the original draft, as well as writing the review and editing. Pascal Oswald contributed to funding acquisition, project administration, resources, supervision, validation, and writing the review and editing. Othmane Mirinioui contributed to the conceptualization, data curation, formal analysis, investigation, methodology, visualization, and writing the review and editing.

Funding: This research received no external funding

Conflicts of Interest: The views expressed in this paper are those of the authors and do not necessarily reflect the views and policies of Natixis CIB or any other organisation

Appendix A. Change of Probability Measure via a Numéraire

In this appendix, we outline an essential technique for pricing fixed-income derivatives: the change in the probability measure via a numéraire. Specifically, we focus on two fundamental probability measures used throughout this paper: the terminal probability measure and the level probability measure. To formalize this framework, we state Theorem A1 of numéraire change, which establishes the transformation between these measures. For additional details, proofs, and practical implications, we refer the reader to [50].

We consider a filtered probability space $(\Omega, \mathcal{F}, (\mathcal{F}_t)_{t \in [0, T]}, \mathbb{Q})$, where \mathbb{Q} represents the risk-neutral probability measure.

In practice, a numéraire serves as a unit of reference when pricing a financial asset.

Definition A1. A numéraire $(N_t)_{t \in [0, T]}$ is any strictly positive (\mathcal{F}_t) -adapted stochastic process such that its discounted value process $(D(0, t)N_t)_{t \in [0, T]}$ is an (\mathcal{F}_t) martingale under probability measure \mathbb{Q} .

For any numéraire $(N_t)_{t \in [0, T]}$, we can define the associated forward probability measure \mathbb{Q}^N by its Radon–Nikodym derivative:

$$\frac{d\mathbb{Q}^N}{d\mathbb{Q}} = D(0, T) \frac{N_T}{N_0}, \quad (\text{A1})$$

Pricing financial derivatives is generally formulated as the calculation of a risk-neutral expectation of a given payoff G discounted by the risk-free rate. The change in numéraire in pricing corresponds to transitioning from the risk-neutral probability measure \mathbb{Q} to the forward probability measure \mathbb{Q}^N . By Girsanov's theorem, we have the following result:

Theorem A1. Given a numéraire $(N_t)_{t \in [0, T]}$, the price at time 0 of a financial derivative with a \mathbb{Q} -integrable payoff G at terminal time T is given by:

$$\mathbb{E}^{\mathbb{Q}}[D(0, T) G] = N_0 \mathbb{E}^{\mathbb{Q}^N} \left[\frac{G}{N_T} \right]. \tag{A2}$$

Moreover, if (W_t) is a \mathbb{Q} -Brownian motion, then the process (W_t^N) is a \mathbb{Q}^N -Brownian motion, which is defined by:

$$dW_t^N = dW_t - \frac{1}{N_t} dN_t \cdot dW_t \tag{A3}$$

In this paper, we use this theorem for two specific numéraires:

1. The price of a zero-coupon bond $B(t, T)$ can serve as a numéraire, and the associated forward probability measure is the terminal probability measure, denoted by \mathbb{Q}^T .
2. The level associated to a swap rate or a European swaption also acts as a numéraire, and the corresponding forward probability measure is called the level probability measure, denoted by \mathbb{Q}^{LVL} .

Appendix B. Numerical Specifications

In this appendix, we briefly present the supplementary data used in the conducted numerical tests described in Section 5.

First, we used the initial zero-coupon rates data presented in Table A1 to construct the entire curve by a cubic-spline interpolation of 3 degrees.

Table A1. Initial zero-coupon rate data.

Tenor	1M	6M	1Y	2Y	3Y	4Y	5Y	6Y	7Y	10Y	15Y	20Y
Rate	3%	2%	2%	2%	3%	3%	3%	3%	4%	4%	5%	5%

Next, for the Monte Carlo simulations, we simulated the Gaussian variable X_t in the LGM-1F model using Formula (45). Numerically, the samples were generated by function `random.normal` in the Python library `numpy`. Along with the interpolated initial zero-coupon rates, we obtained the simulated zero-coupon bonds curves (at a future date) using reconstruction Formula (??). The numerical parameters of the LGM-1F are reported in Table A2, and we highlight that we used a constant volatility in our numerical tests.

Table A2. LGM-1F model parameters.

Mean Reversion λ	Volatility σ
1%	0.5%

The risk profile characteristic of the counterparty, used in all our calculations of the credit value adjustment (CVA), is characterized by the recovery rate and the constant default intensity reported in Table A3.

Table A3. Counterparty risks profile characteristics.

Recovery Rate R	Default Intensity μ
1%	0.5%

We report in Table A4 the characteristics of the interest rate swap portfolio used in our numerical tests. Except the notional and the start date, the parameters of the portfolio were chosen randomly based on predefined ranges or specific sets of values. Specifically, the maturity was selected as a semi-integer value between 1 year and 7 years; the frequency

was chosen to be semiannual, quarterly, or annual; the fixed rate was selected from the range of 2% to 5%; and the type was assigned as either a receiver or a payer swap. This randomized selection ensured a diverse and representative portfolio of interest rate swaps in the bank.

Table A4. The characteristics of the swaps in the portfolio used for numerical tests.

Deal ID	Start Date	Frequency	Notional	Fixed Rate	Maturity	Type
0	0	0.25	10,000	4%	2.5	Payer
1	0	0.25	10,000	5%	1	Payer
2	0	0.25	10,000	5%	1	Payer
3	0	0.5	10,000	3%	7	Receiver
4	0	1	10,000	4%	6.5	Payer
5	0	1	10,000	3%	4.5	Payer
			⋮			
395	0	0.5	10,000	4%	4.5	Receiver
396	0	1	10,000	2%	2.5	Payer
397	0	0.5	10,000	4%	5.5	Payer
398	0	1	10,000	4%	3.5	Payer
399	0	0.25	10,000	3%	4.5	Payer

Finally, Gaussian process regression and Bayesian quadrature were implemented using the Python libraries *GPY* and *emukit*, respectively. Both methods utilized a squared exponential kernel (10), with its initial (before training) numerical parameters reported in Table A5. For Bayesian quadrature, integration was performed with respect to the Lebesgue measure on the interval $[0, T]$, as the survival probabilities were deterministic and straightforward to compute.

Table A5. Squared exponential kernel parameters used for GPR and Bayesian quadrature.

Variance σ_f	Length Scale l
1%	10%

The inputs and numerical specifications detailed in this appendix are provided as a complementary resource to enhance the understanding of the implementation and results presented in Section 5. These details ensure the transparency and reproducibility of the methodologies and results discussed in the main text.

References

- Green, A. *XVA: Credit, Funding and Capital Valuation Adjustments*; John Wiley & Sons: Hoboken, NJ, USA, 2015.
- Gregory, J. *Counterparty Credit Risk and Credit Value Adjustment: A Continuing Challenge for Global Financial Markets*; John Wiley & Sons: Hoboken, NJ, USA, 2012.
- Hoffman, F. *Credit Valuation Adjustment*, Oxford University, Mathematical Institute, 2011.
- Basel Committee on Banking Supervision. *Basel III: A Global Regulatory Framework for More Resilient Banks and Banking Systems*; Technical report; 2010; Revised June 2011.
- Basel Committee on Banking Supervision. *Minimum Capital Requirements for Market Risk*; Technical report; Bank for International Settlements, Basel, Switzerland, 2019.
- Basel Committee on Banking Supervision. *Credit Valuation Adjustment Risk: Targeted Final Revisions - Consultative Document*; Technical report; Bank for International Settlements, Basel, Switzerland, 2020.
- Sokol, A. *Learning Quantitative Finance with R: From Models to Applications*; Packt Publishing: Birmingham, UK, 2016.
- Hull, J.C. *Risk Management and Financial Institutions*; John Wiley & Sons: Hoboken, NJ, USA, 2014.
- Rockafellar, R.T.; Uryasev, S. Optimization of Conditional Value-at-Risk. *J. Risk* **2000**, *2*, 21–42.
- Abad, P.; Benito, S.; Lopez, C. A Comprehensive Review of Value at Risk Methodologies. *Span. Rev. Financ. Econ.* **2013**, *12*, 15–32. <https://doi.org/10.1016/j.srfe.2013.06.001>.
- Dowd, K. *An Introduction to Market Risk Measurement*; John Wiley & Sons: Hoboken, NJ, USA, 2003.
- Duffie, D.; Pan, J. An Overview of Value at Risk. *J. Deriv.* **1997**, *4*, 7–49.

13. Lichters, R.; Stamm, R.; Gallagher, D. *Modern Derivatives Pricing and Credit Exposure Analysis: Theory and Practice of CSA and XVA Pricing, Exposure Simulation and Backtesting*; Applied Quantitative Finance; Palgrave Macmillan: London, UK, 2015.
14. Liu, Q. Calculation of Credit Valuation Adjustment Based on Least Square Monte Carlo Methods. *Math. Probl. Eng.* **2015**, *2015*, 1–6. <https://doi.org/10.1155/2015/959312>.
15. on Banking Supervision, B.C. *Fundamental Review of the Trading Book: A Revised Market Risk Framework—Consultative Document*; Technical report; Bank for International Settlements, Basel, Switzerland, 2013.
16. Zeron-Medina, M.; Ruiz, I. *Denting the FRTB IMA Computational Challenge via Orthogonal Chebyshev Sliding Technique*; Risk Books: London, UK, 2021.
17. Swaps, I.; International Swaps and Derivatives Association (ISDA), D.A. *User's Guide to the ISDA Credit Support Documents under English Law*; Technical report; International Swaps and Derivatives Association, New York, USA, 1999.
18. Crépey, S.; Dixon, M. Gaussian Process Regression for Derivative Portfolio Modeling and Application to CVA Computations. *arXiv* **2019**, arXiv:1901.11081.
19. Gonzalez, J.; Lezmi, E.; Roncalli, T.; Xu, J. Financial Applications of Gaussian Processes and Bayesian Optimization. *arXiv* **2019**, arXiv:1903.04841.
20. Qian, F. Advanced Estimation of Credit Valuation Adjustment. Ph.D. Thesis, Delft University of Technology, Delft, The Netherlands, 2017.
21. Mu, G.; Godina, T.; Maffia, A.; Sun, Y.C. Supervised Machine Learning with Control Variates for American Option Pricing. *Found. Comput. Decis. Sci.* **2018**, *43*, 207–217.
22. Sambasivan, R.; Das, S. A Statistical Machine Learning Approach to Yield Curve Forecasting. In Proceedings of the 2017 International Conference on Computational Intelligence in Data Science (ICCIDS), Chennai, India, 2–3 June 2017; IEEE: Piscataway, NJ, USA, 2017; pp. 1–6.
23. Buehler, H.; Gonon, L.; Teichmann, J.; Wood, B. Deep Hedging. *Quant. Financ.* **2019**, *19*, 1271–1291. <https://doi.org/10.1080/14697688.2019.1571683>.
24. Culkun, R.; Das, S.R. Machine Learning in Finance: The Case of Deep Learning for Option Pricing. *J. Invest. Manag.* **2017**, *15*, 92–100.
25. DeBrusk, C.; Du, E. *Why Wall Street Needs to Make Investing in Machine Learning a Higher Priority*; Technical report; Oliver Wyman: New York, NY, USA, 2018.
26. (Financial Stability Board (FSB) *Artificial Intelligence and Machine Learning in Financial Services—Market Developments and Financial Stability Implications*; Technical report (<https://www.fsb.org/2017/11/artificial-intelligence-and-machine-learning-in-financial-service/>) 2017.
27. Leo, M.; Sharma, S.; Maddulety, K. Machine Learning in Banking Risk Management: A Literature Review. *Risks* **2019**, *7*, 29.
28. Wilkens, S. Machine Learning in Risk Measurement: Gaussian Process Regression for Value-at-Risk and Expected Shortfall. *J. Risk Manag. Financ. Institutions* **2019**, *12*, 374–383.
29. Cao, J.; Chen, J.; Hull, J.; Poulos, Z. Deep Hedging of Derivatives Using Reinforcement Learning. *arXiv* **2021**, arXiv:2103.16409.
30. De Spiegeleer, J.; Madan, D.B.; Reyners, S.; Schoutens, W. Machine Learning for Quantitative Finance: Fast Derivative Pricing, Hedging and Fitting. *Quant. Financ.* **2018**, *18*, 1635–1643.
31. Leh dili, N.; Oswald, P.; Guéneau, H. Market Risk Assessment of a Trading Book Using Statistical and Machine Learning. 2019. <https://doi.org/10.13140/RG.2.2.23796.71047>.
32. Ruiz, I.; Zeron, M. *Machine Learning for Risk Calculations: A Practitioner's View*; John Wiley & Sons: Hoboken, NJ, USA, 2021.
33. Glau, K.; Mahlstedt, M.; Pötz, C. A New Approach for American Option Pricing: The Dynamic Chebyshev Method. *SIAM J. Sci. Comput.* **2019**, *41*, B153–B180.
34. Pykhtin, M.; Rosen, D. *Pricing Counterparty Risk at the Trade Level and CVA Allocations*; Technical report, FEDS Working Paper; FEDS: Washington, DC, USA, 2010.
35. Jooma, Y.; Liu, H. *GARP Research Fellowship 2017: An Analysis of the ISDA Model for Calculating Initial Margin for Non-Centrally Cleared OTC Derivatives*; Technical report; 2018.
36. Bielecki, T.; Brigo, D.; Patras, F. *Credit Risk Frontiers: Subprime Crisis, Pricing and Hedging, CVA, MBS, Ratings, and Liquidity*; John Wiley & Sons: Hoboken, NJ, USA, 2011.
37. Chen, Z.; Naslidnyk, M.; Gretton, A.; Briol, F.X. Conditional Bayesian Quadrature. *arXiv* **2024**, arXiv:2406.16530.
38. Gessner, A. *Numerical Integration as and for Probabilistic Inference*; Universität Tübingen: Tübingen, Germany, 2022.
39. Kanagawa, M.; Sriperumbudur, B.K.; Fukumizu, K. Convergence Guarantees for Kernel-Based Quadrature Rules in Misspecified Settings. *arXiv* **2016**, arXiv:1605.07254.
40. Osborne, M.; Garnett, R.; Ghahramani, Z.; Duvenaud, D.K.; Roberts, S.J.; Rasmussen, C. Active Learning of Model Evidence Using Bayesian Quadrature. In Proceedings of the Advances in Neural Information Processing Systems, Lake Tahoe, NV, USA, 3–6 December 2012; Volume 25.
41. Williams, C.K.I.; Rasmussen, C.E. *Gaussian Processes for Machine Learning*; MIT Press: Cambridge, MA, USA, 2006; Volume 2.
42. Cheyette, O. Markov Representation of the Heath-Jarrow-Morton Model. *SSRN Electron. J.* **2001**, 1–12. <https://doi.org/10.2139/ssrn.6073>.
43. Mercurio, F.; Brigo, D. *Interest Rates Models Theory and Practice: II, Continuous Time Models*; John Wiley & Sons: Hoboken, NJ, USA, 2008.

44. Forrester, A.I.J.; Sóbester, A.; Keane, A.J. Multi-fidelity optimization via surrogate modelling. *Proc. R. Soc. A Math. Phys. Eng. Sci.* **2007**, *463*, 3251–3269.
45. Peherstorfer, B.; Willcox, K.; Gunzburger, M. Survey of multifidelity methods in uncertainty propagation, inference, and optimization. *SIAM Rev.* **2018**, *60*, 550–591.
46. Kennedy, M.C.; O’Hagan, A. Predicting the output from a complex computer code when fast approximations are available. *Biometrika* **2000**, *87*, 1–13.
47. Le Gratiet, L.; Cannamela, C.; Iooss, B. Bayesian analysis of multi-fidelity data: Gaussian processes and hierarchical models. *Bayesian Anal.* **2013**, *9*, 37–58.
48. Li, Y. Utilisation Des Méta-Modèles Multi-Fidélité pour l’Optimisation De La Production Des Réservoirs. Ph.D. Thesis, Université de Pau et des Pays de l’Adour, Pyrénées-Atlantiques, France, 2016. Thesis.
49. Mirinioui, O. Bayesian Quadrature and Multi-Fidelity Machine Learning for Financial Risk Metrics Calculation. Master’s Thesis, University Paris-Dauphine, Paris, France, 2024.
50. Privault, N. *Introduction to Stochastic Finance with Market Examples*, 2nd ed.; Chapman & Hall/CRC: Boca Raton, FL, USA, 2022; pp. 565–600.

Disclaimer/Publisher’s Note: The statements, opinions and data contained in all publications are solely those of the individual author(s) and contributor(s) and not of MDPI and/or the editor(s). MDPI and/or the editor(s) disclaim responsibility for any injury to people or property resulting from any ideas, methods, instructions or products referred to in the content.